American J. of Engineering and Applied Sciences 3 (2): 441-448, 2010
ISSN 1941-7020

Interaction of Soil Static and Dynamic Stiffness and Buried Pipeline Under Harmonic Vibration

[1]Alireza Mirza Goltabar Roshan, [2]Hossein Khalilpasha and [1]Mohsen Ghorbani
[1]Department of Civil Engineering,
Babol Noushirvani University of Technology, Iran
[2]School of Civil Engineering, The University of Queensland, Australia

Abstract: Problem statement: When earthquake is occur, many damages were occurred in pipelines that San Francisco (1906) and Manson (1908), Kobe (Japan) and ate are samples of this topic. So many researchers studied on the pipelines and dynamic forces. **Approach:** Determine static and dynamic performance parameters of the pipeline and the surrounding soil such as static stiffness, dynamic stiffness, damping and additional mass share of soil which take part with pipe mass in dynamic performance. In the static case relationship between friction forces and joint deflections in a buried element pipe had be calculated and with using of some experimental results and results are compared together. For dynamic cases, Dynamic equilibrium equation of pipeline element axial vibration in continuous system, with neglecting the effect of soil mass share which participates in producing vibration and with considering of it were abstained and values of displacement and forces were calculated. In continuous, these formulations were process for many cases and were drawn in graphs for comparison. **Results:** Stiffness for $\omega/\omega_{n<1}$ doesn't change much but for the values more than 1 it increase rising. when $\omega/\omega_{n<1}$ the ratio of dynamic stiffness to the static stiffness is less than unique except in big amount of damping ratio ($\rho>0.5$) which the ratio becomes more than 1. Finally for $\omega/\omega_{n>1}$, the ratio of dynamic to static stiffness rises rapidly and by increasing the additional mass, the value of dynamic stiffness in case of $\omega/\omega_{n>1}$ would increase highly. **Conclusion:** The static performance between soil and pipe is nonlinear in axial direction and when the hysteric dominates grows, the value of force dominates between soil and pipe and dynamic stiffness would ascend. Also by increasing damping ratio, the dynamic stiffness would increase too however it depends on the static to dynamic stiffness ratio and the damping ratio.

Key words: Interaction, pipeline, axial, dynamic, vibration

INTRODUCTION

The purpose of this study is to study on the static and dynamic properties of buried pipeline and surrounded soil in axial direction due to harmonic dynamic vibration. The stiffness between soil and pipe in different static and dynamic conditions and cases based on the dynamic distributed formulation, considering soil additional mass share and also refer to numerical experimental results, has been estimated and concluded in the following pages.

Poulos and Sim (1979) has presented a method applying elastic theory that axial vibration loading of a pile would increase the porous pressure, decrease the soil modulus and lateral resistance of soil. A quasi-bifurcation theory of dynamic buckling and a simple flow theory of plasticity are employed to analyze the axisymmetric, elastic-plastic buckling behavior of buried pipelines subject to seismic excitations. Using the seismic records of the 1971 San Fernando earthquake, a series of numerical results have been obtained, which show that, at strain rates prevalent in earthquakes, the dynamic buckling axial stress or strain of a buried pipe is only slightly higher than that of static buckling (Lee, 1984).

A comparative study has been performed to obtain the response characteristics of strains in a buried pipeline section, axial relative displacement and transverse relative displacement. The maximum relative displacement response in the transverse direction is significant even under the design level of earthquakes. The maximum transverse displacement response mainly occurs at the center of the pipeline and shows that the pipeline embedded in soft clay is particularly

Corresponding Author: Alireza Mirza Goltabar Roshan, Department of Civil Engineering,
Babol Noushirvani University of Technology, Iran

vulnerable to earthquake excitation. A minor discrepancy is observed between the responses of the pipeline with various angles of lowering and highering bends. In all, the soil type is significant for the response of the pipeline (Do *et al*., 2009).

The axial performance of pile is approximately close to buried pipeline. The pile under axial static load resists against the loading with side strength in pile column and end pile strength at the end edge of pile. At this research, resistance between pile and surrounding soil is modeled according to Winkler theory with elastic springs. Then, the formulation and experimental methods, to find a method for determining dynamic stiffness (impedance function), damping between the pile and surrounding soil and also the additional mass of soil which contributes with pile in dynamic performance applying harmonic vibration would be presented. The formulation methodology is based on dynamic of structures theory and mechanical vibration theory in time and frequency space applying Fourier transport. An efficient numerical approach based on both boundary and finite element methods is developed in this work. This development is capable of realistic three dimensional analyses of soil-structure interaction problems in the real time domain and is specifically tailored to buried lifelines. Results are gauged against empirical design formulae. It is shown that the seismically induced stress state in a buried pipeline is more pronounced in the case of transverse vibrations than in the case of longitudinal vibrations (Manolis *et al*., 1995). Study on the Dynamic responses of buried pipelines during a liquefaction (Wang *et al*., 1990) and subsea pipeline buckling (Neil and Tran, 1996) were done by other researchers.

MATERIALS AND MATHODS

In this research, with using of experimental results which was done by first author, static and dynamic stiffness were calculated in two methods that are explained in later section. Experiment data are for many cases of pipe depth and water absorption. In continuo, with using of formulation, variation of dynamic and static stiffness, mass of pipe, the part of soil which contributes with pipe in dynamic performance, ratio of frequency to natural frequency and damping ratios are compared together.

Study the interaction of soil and pipe in static case: The relationship between friction forces and joint deflections in a buried element pipe can be shown as Eq. 1:

$$\Delta F_i = \frac{E_p A_p}{L_1}\left(u_{i-1} - 2u_i + u_{i+1}\right) \quad (1)$$

u_i and u_{i+1} are the measured displacements in points i and i+1 of pipe length in laboratory.

At this part, the axial stiffness between the soil and pipe has been calculated by Calton and experimental method. In Calton method, the values of stiffness have been estimated by dividing the force values to initial deflections. Sample result of Calton method is shown in Table 1.

Here is a sample of calculation in experimental method:

$$\Delta u_1 = 0.13 - 0.10 = 0.03\,\text{mm}\ ,\ \Delta u_2 = 0.10 - 0.09 = 0.01\,\text{mm}$$

$$\Delta u_3 = 0.09 - 0.07 = 0.02\ \text{mm},$$

$$\Delta u_4 = 0.07 - 0.045 = 0.025\ \text{mm}$$

$$\Delta u_5 = 0.045 - 0.02 = 0.025\ \text{mm}$$

Mean value of relative deflection = 0.022 mm:

$$\Delta F = \frac{131.1}{6} \times \frac{135}{122} = 24.16\ \text{Kg}$$

Thus:

$$K_s = \frac{24.16 - 0}{0.022 - 0} = 1098.\frac{\text{Kg}}{\text{mm}}$$

The calculated number is for the initial modulus. The second modulus stiffness can be calculated as below:

$$\Delta u_1 = 0.56 - 0.53 = 0.03\,\text{mm}\ ,\ \Delta u_2 = 0.53 - 0.48 = 0.05\,\text{mm}$$
$$\Delta u_3 = 0.48 - 0.41 = 0.07\,\text{mm}\ ,\ \Delta u_4 = 0.41 - 0.25 = 0.16\,\text{mm}$$
$$\Delta u_5 = 0.25 - 0.09 = 0.16\,\text{mm}$$

Mean value of relative deflection = 0.094 mm:

$$\Delta F = \frac{154.6}{6} \times \frac{135}{122} = 28.51\ \text{Kg}$$

135/122 is the transformation coefficient:

$$K_s = \frac{28.51 - 24.16}{0.094 - 0.022} = 60.4\frac{\text{Kg}}{\text{mm}}$$

Table 1: Calculation of static stiffness for an experiment by Calton method

	Coleon	
Ks (Kg mm^{-2})	Deflection (mm)	Force (Kg)
1115.92	0.13	145.07
305.49	0.56	171.07

Table 2: Calculation of static stiffness for an experiment by experimental method

			Experimental method				
k_s	F	u	u_5-u_6	u_4-u_5	u_3-u_4	u_2-u_3	u_1-u_2
1098.01	24.18	0.022	0.025	0.025	0.02	0.01	0.03
60.4	28.51	0.094	0.160	0.160	0.07	0.05	0.03
19.8	29.66	0.148	0.295	0.295	0.04	0.06	0.05

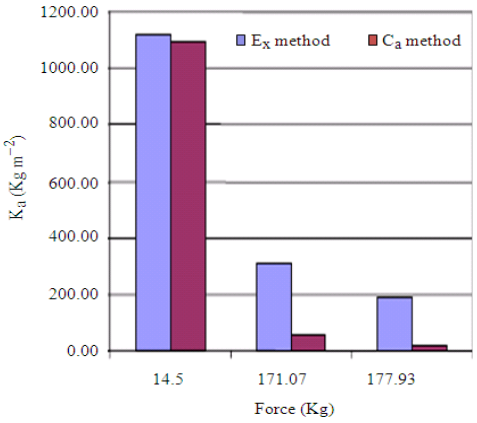

Fig. 1: Comparison of calculated stiffness by two methods in an experiment

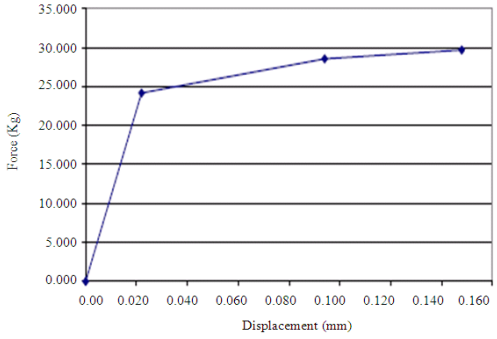

Fig. 2: Force-displacement curve for an experiment

and also for the third modulus, we have:

$$\Delta u_1 = 0.95 - 0.90 = 0.05\,\text{mm}\,,\ \Delta u_2 = 0.9 - 0.84 = 0.06\,\text{mm}$$

$$\Delta u_3 = 0.84 - 0.80 = 0.06\ \text{mm}\,,\ \Delta u_4 = 0.80 - 0.50 = 0.30\ \text{mm}$$

$$\Delta u_5 = 0.50 - 0.21 = 0.29\ \text{mm}$$

Mean value of relative deflection = 0.152 mm:

$$\Delta F = \frac{160.6}{6} \times \frac{135}{122} = 29.66\ \text{Kg}$$

Thus:

$$K_s = \frac{29.66 - 28.51}{0.152 - 0.094} = 19.8 \frac{\text{Kg}}{\text{mm}}$$

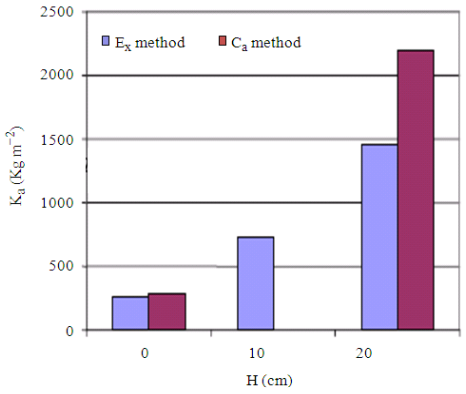

Fig. 3: Calculation of stiffness for different height of soil over the pipe (water absorption 2.97%)

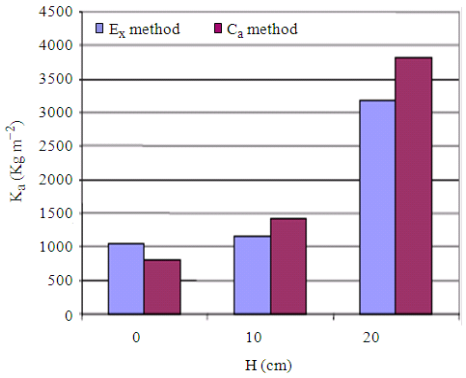

Fig. 4: Calculation of stiffness for different height of soil over the pipe (water absorption 10.2%)

Calculation of static stiffness for an experiment by experimental method is shown in Table 2 and Comparison of calculated stiffness by two methods in an experiment is shown in Fig. 1. Also force-displacement curve for an experiment is shown in Fig. 2.

Effect of the height of the soil over the pipe to the axial stiffness: To study the effect of the height of the soil over the pipe, it has been assumed that all of the conditions are constant and just the height of the soil has changed. It means that, a PVC pipe with diameter of 26 cm and 4 mm thickness has been put in a sand soil with water absorption percentage of 2.97 and one pas compaction. The values of stiffness have been

calculated for different heights of 0, 10 and 20 cm. Figure 3 shows the value of stiffness for different heights. Also the process has been done for a different water absorption of 10.2% which is indicated in Fig. 4. Figure 3 and 4 indicates that when the depth of the soil increases, the stiffness of the soil increases in both methods too. The main reason for increase in stiffness is increasing the lateral pressure to the pipeline and then producing stronger friction forces between soil and pipe. Also, by increasing the water absorption percentage of the soil, the value of stiffness would increase too.

Interaction of soil and pipeline in dynamic condition under harmonic vibration: Dynamic equilibrium equation of pipeline element axial vibration in continuous system, neglecting the effect of soil mass share which participates in producing vibration can be formulated as Eq. 2:

$$\rho_p A_p \frac{d^2u(x,t)}{dt^2} - E_p A_p \frac{d^2u(x,t)}{dx^2} + C_a \frac{du(x,t)}{dt} + K_a u(x,t) = K_a u_g(x,t) \quad (2)$$

Equation 2 illustrates the governing equation of a continuous system that applying the boundary and initial conditions and solving the corresponding deferential equation, the displacement function u (x,t) can be obtained up to constant values of k_a, axial stiffness between soil and pipe, ρ_p special mass of pipe, E_p pipe elasticity modulus, A_p pipe section area and C_a axial damping of soil and pipe.

The dynamic equilibrium equation can be shown in discrete system with multi degree of freedom considering external forces and excluding ground motion as Eq. 3:

$$[M]\{\ddot{u}\} + [C]\{\dot{u}\} = \{f(t)\} \quad (3)$$

The axial dynamic equilibrium in the discrete system with two degree of freedom considering additional mass of soil (M_{add}) can be shown as Eq. 4:

$$\begin{bmatrix} M_p + M_{add} & 0 \\ 0 & M_p + M_{add} \end{bmatrix} \begin{bmatrix} \ddot{u}_1 \\ \dot{u}_2 \end{bmatrix} + \begin{bmatrix} C_1 & 0 \\ 0 & C_2 \end{bmatrix} \begin{bmatrix} \ddot{u}_1 \\ \dot{u}_2 \end{bmatrix} + \begin{bmatrix} K_{11} & K_{12} \\ K_{21} & K_{22} \end{bmatrix} \begin{bmatrix} \ddot{u}_1 \\ \dot{u}_2 \end{bmatrix} = \begin{bmatrix} f_1(t) \\ f_2(t) \end{bmatrix} \quad (4)$$

Where:

M_p = The mass of pipe
M_{add} = The part of soil which contributes with pipe in dynamic performance
u_i, $\dot{u}_i$, $\ddot{u}_i$ = Displacement, velocity and equivalent joint acceleration in joint i
C_i = the equivalent damping in joint i
k_{ij} = The stiffness in joint i to the effect of joint j
$f_i(t)$ = The equivalent force in joint i

Most of the researchers neglect the effect of M_{add} because of its tiny value but it has been considered at this study. Equation 3 can be distributed for more than two degree of freedom. In such a case that Eq. 3 changes to Eq. 5 the factor k_d is defined as dynamic stiffness or impedance function:

$$[K_d]\{u(t)\} = \{f(t)\} \quad (5)$$

In a single degree of freedom case the frequency dominates impedance function can be shown as Eq. 6:

$$K_d(\omega) = -\omega^2(M_p + M_{add}) + K + i\omega c \quad (6)$$

ω is angular frequency and $k_d(\omega)$ and $k_d(t)$ are the foriour transform of each other. Thus they transform the frequency space to the time space and vise versa and are compatible with Eq. 7:

$$k_d(t) = \int_{-\infty}^{\infty} k_d(\omega) e^{i\omega t} d\omega$$
$$k_d(\omega) = \frac{1}{2\pi} \int_{-\infty}^{\infty} k_d(t) e^{-i\omega t} dt \quad (7)$$

The same as the relation between $k_d(t)$ and $k_{ad}(\omega)$, displacement u(t) in time space and displacement in frequency space u(ω) and also force f(t) in time space with force in frequency space f(ω) can be related to each other by fourier transform as Eq. 8:

$$U(\omega) = \frac{1}{2\pi} \int_{-\infty}^{\infty} u(t) e^{-i\omega} dt \quad u(t) = \int_{-\infty}^{\infty} U(\omega) e^{i\omega t} d\omega \quad (8)$$

According to theory of dynamics of structures and fundamental of mechanical vibration and random vibration viewpoint, the dynamic stiffness $k_d(t)$ in time dominant is the result of the problem due to unique impulse, that applying Fourier transform the frequency response of the system or the dynamic stiffness in time dominant would be determined. Frequency dominant dynamic parameters are the Fourier transform of time dominant dynamic parameters and hence the frequency space can be transformed to time frequency by Fourier transforms and vise versa.

In static case, the equivalent dynamic stiffness can be determined as static stiffness $k_d(\omega) = k$. Then the

numerical value of dynamic stiffness can be shown as Eq. 9:

$$\frac{F_{\bullet}}{U_{\bullet}} = |K_d(\omega)| = K\sqrt{[1-(\frac{\omega}{\omega_n})^2 + [2\rho(\frac{\omega}{\omega_n})]^2} \quad (9)$$

Equation 9 can be drawn as a graph for different values of damping ratios (ρ) and different values for the division of hysteric frequency to natural frequency. The minimum of dynamic stiffness is produced when $\omega = \omega_n$ and by increasing damping ratio the dynamic stiffness would increase too. For impacting the pile to the ground or penetration of a stick in the ground it can be assumed that $\omega = \omega_n$ that ground dynamic stiffness would be in the minimum value. When $\omega<\omega_n$ the condition would decline to static and when $\omega>\omega_n$ dynamic stiffness would increase a lot. When M_{add} participates in the equation, because it is a function of ω, Ø, c, ω_n, M_p, the equation would be a complex equation. In fact M_{add} becomes a function of ω_n and ω_n becomes a function of M_{add}. According to the different conditions of $\omega<\omega_n$ and $\omega>\omega_n$ small ρ (under critical) and big ρ(super critical) and also with or without M_{add} the dynamic stiffness would be determined and drawn.

To consider the effect of additional mass, it should be considered that, natural frequency of a single degree of freedom system with additional mass can be defined as Eq. 10:

$$\omega_n = \sqrt{\frac{K}{M}} = \sqrt{\frac{K}{M_p + M_{add}}} \quad (10)$$

If we assume that the additional mass is equal to 0.5 M_p and M_p, the value of natural frequency is equal to $(1/\sqrt{1.5})\ \omega_n$, $(1/\sqrt{2})\ \omega_n$. It can be said that the natural frequency is dependent on the mass of pile and additional mass. When M_{add} interferes a complete couple equation would be produced because M_{add} is function of hysteric frequency, phase changing angle, harmonic force dominant and harmonic displacement dominant and the natural frequency is a function of M_{add}. in the other hand Eq. 11 is available:

$$\phi = \tan^{-1}\frac{c\omega}{K - m\omega^2}$$
$$K(\omega) = \frac{F_0}{u_0}(\cos\phi + i\sin\phi) \quad (11)$$

If the dynamic force represents as a harmonic force, displacement would be harmonic too but with a phase delay:

$$F(t) = F_0\sin(\omega t) \quad (12)$$

$$u(t) = u_0\sin(\omega t - \phi) \quad (13)$$

That Φ is output phase delay (displacement) in relation to input (dynamic force). The relation between F_0 and u_0 can be defined as Eq. 14:

$$u_0 = \frac{F_0}{K\sqrt{\left[1-\left(\frac{\omega}{\omega_n}\right)^2\right]^2 + \left[2\rho\left(\frac{\omega}{\omega_n}\right)\right]^2}} \quad (14)$$

Where:

$$\rho = \frac{C}{2m\omega_n}$$

If we consider $u_{st} = \frac{F_0}{K}$ (that is static displacement). Then:

$$\frac{u_0}{u_{st}} = \frac{u_{dy}}{u_{st}} = \frac{1}{\sqrt{\left[1-\left(\frac{\omega}{\omega_n}\right)^2\right]^2 + \left[2\rho\left(\frac{\omega}{\omega_n}\right)\right]^2}} \quad (15)$$

Hence the value of dynamic stiffness is equal to:

$$\frac{F_0}{u_0} = |K_d(\omega)| = K\sqrt{\left[1-\left(\frac{\omega}{\omega_n}\right)^2\right]^2 + \left[2\rho\left(\frac{\omega}{\omega_n}\right)\right]^2} \quad (16)$$

The Eq. 15 and 16 can be draw as a graph for different values of ρ and (ω/ω_n).the numerical value of it would be constant always.

The variation of dynamic stiffness versus ω/ω_n is the reverse of variation of dynamic displacement versus ω/ω_n up to the value of damping; the maximum value has a little distance from ω/ω_n point. If M_{add} is considered, the distance would increase, because the situation of ω_n would change in that case.

Although Eq. 16 is for a harmonic force and displacement, but is different from the real conditions because it doesn't interfere the value of M_{add}. But it can be used for stating the numerical values of dynamic stiffness. The availability of M_{add} is effective in variation of ω_n that by elimination of damping and external force terms, it can not be an ordinary eigen value problem:

$$(m + m_{add})\ddot{x} + C\dot{x} + Kx = f(t) \quad (17)$$

By eliminating C_x and f (t) M_{add} remains dependent to the initial conditions of the problem because ω_n is dependant to M_{add} and ρ. The equations show that the numerical value of dynamic stiffness F_0/u_0 is independent to the amplitude but dependent to the input frequency ω and in the other side ω_n that itself considering the addition of M_{add} is against the ordinary structural dynamics and dependent on the input conditions of problem ω, ρ. In the laboratory the values of F_0, u_0 have been gained and the results are convincing. Experimental results also show that the numerical value of dynamic stiffness is not so sensitive to amplitude but dependent to the input frequency.

The numerical value of dynamic stiffness would never be a negative number because it is summation of quadratic and positive items. As it has been said before M_{add} is function of ω, c, ω_n, m. In the other word M_{add} is a function of ω_n and vise versa. Therefore the dynamics of structures problem should be solved at parallel.

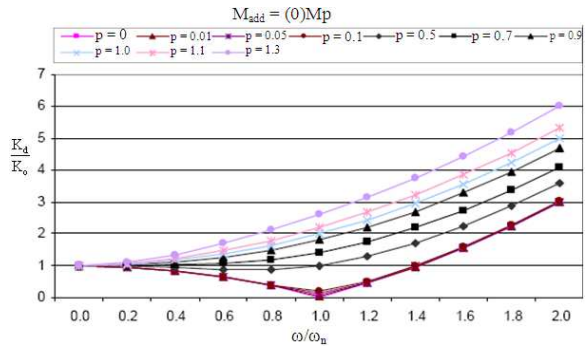

Fig. 5: Variation of K_d/K_0 with ω/ω_n for $M_{add} = 0$

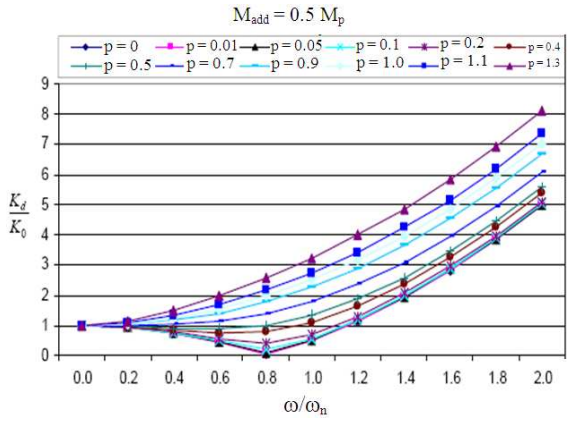

Fig. 6: Variation of K_d/K_0 with ω/ω_n for $M_{add} = 0.5\ M_p$

Table 3 indicates a sample variation of ω/ω_n for $M_{add} = 0$ considering different values for ρ. Figure 5-7 show the variation of dynamic stiffness to static stiffness for the ratio of hysteric frequency to natural frequency and for different values of additional mass and different damping ratios. Figure 8-15 indicate the variation of dynamic stiffness to static stiffness for the ratio of hysteric frequency to natural frequency and for different values of ρ.

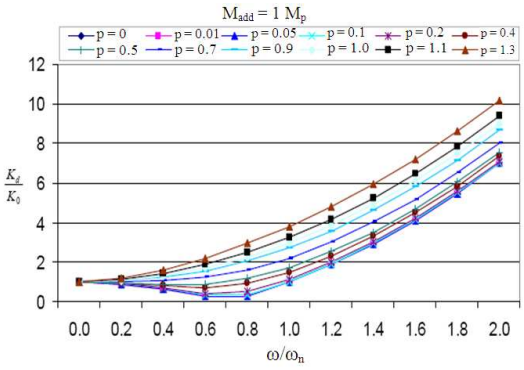

Fig. 7: Variation of K_d/K_0 with ω/ω_n for $M_{add} = 1\ M_p$

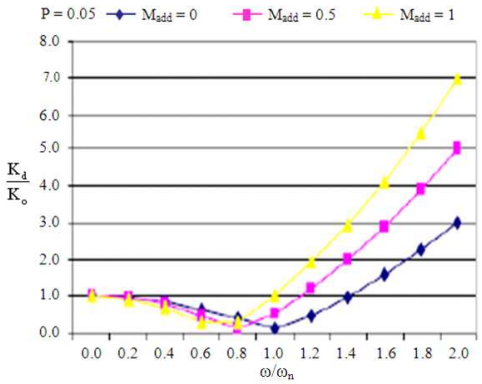

Fig. 8: Variation of K_d/K_0 with ω/ω_n for ρ = 0.05

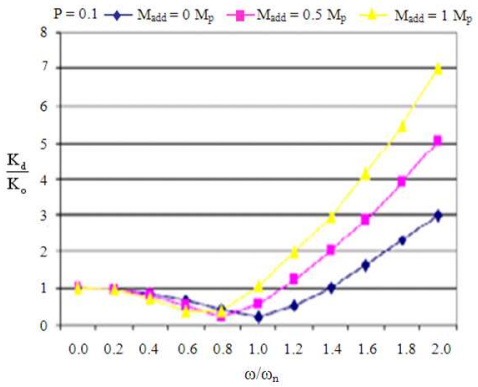

Fig. 9: Variation of K_d/K_0 with ω/ω_n for ρ = 0.1

Table 3: Variation of K_d/K_0 with ω/ω_n for M_{add} = 0 and different ρs

ρ	0	0.01	0.05	0.1	0.2	0.4	0.5	0.7	0.9	1	1.1	1.3
ω/ω_n = 0	1.00	1.00	1.000	1.000	1.000	1.000	1.000	1.00	1.000	1.00	1.000	1.000
ω/ω_n = 0.2	0.96	0.96	0.960	0.961	0.963	0.973	0.981	1.00	1.025	1.04	1.056	1.092
ω/ω_n = 0.4	0.84	0.84	0.841	0.844	0.855	0.899	0.930	0.01	0.106	1.16	1.217	1.337
ω/ω_n = 0.6	0.64	0.64	0.643	0.651	0.684	0.800	0.877	1.06	1.255	1.36	1.467	1.686

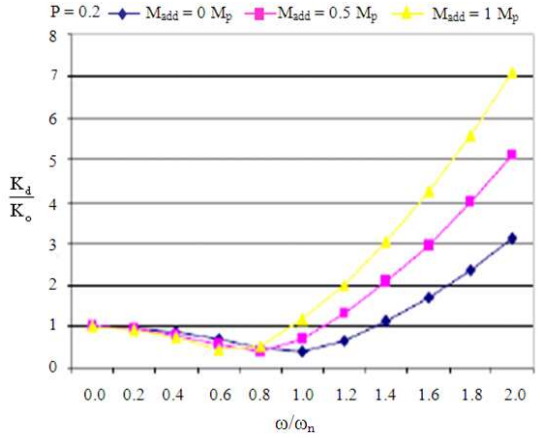

Fig. 10: Variation of K_d/K_0 with ω/ω_n for ρ = 0.2

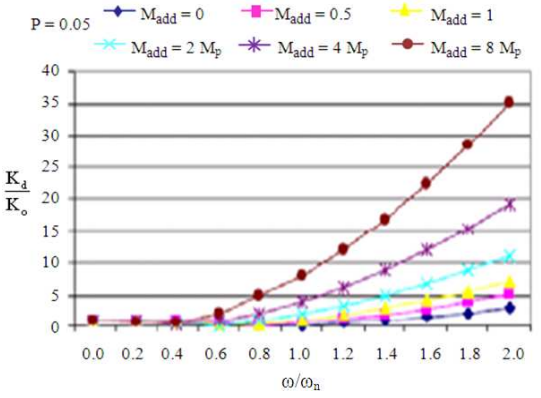

Fig. 11: Variation of K_d/K_0 with ω/ω_n for ρ = 0.4

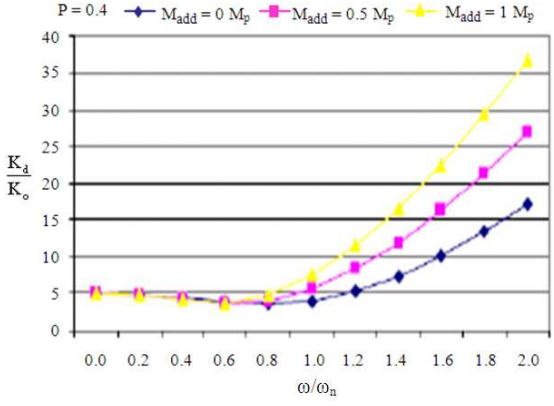

Fig. 12: Variation of K_d/K_0 with ω/ω_n for ρ = 0.05

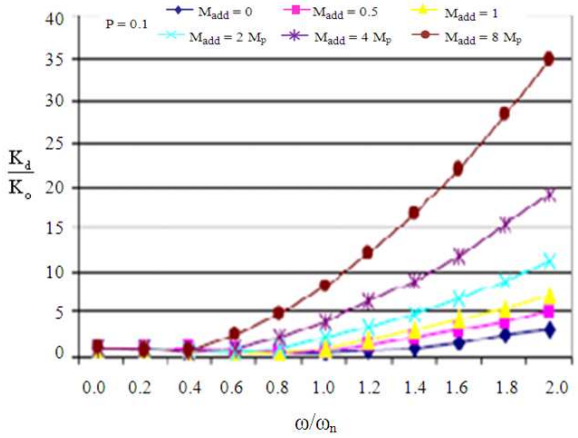

Fig. 13: Variation of K_d/K_0 with ω/ω_n for ρ = 0.1

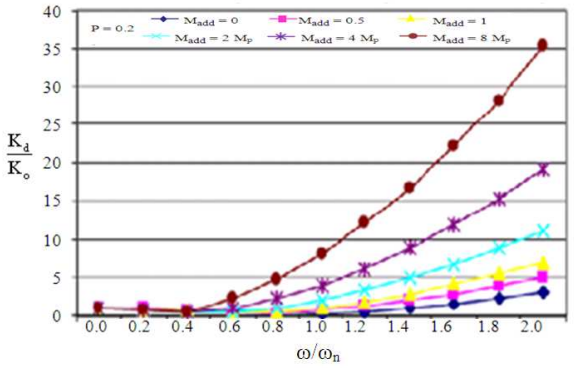

Fig. 14: Variation of K_d/K_0 with ω/ω_n for ρ = 0.2

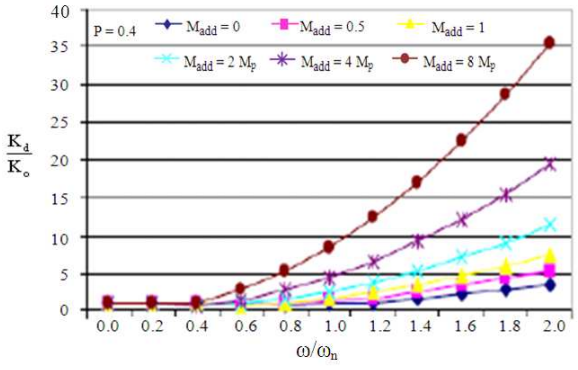

Fig. 15: Variation of K_d/K_0 with ω/ω_n for ρ = 0.4

RESULTS AND DISCUSSION

As it is shown in figures, dynamic stiffness for $\omega/\omega_{n<1}$ doesn't change much but for the values more than 1 it increase rising so that for $\omega/\omega_n = 2$ it becomes multiple. The dynamic stiffness increases by increasing damping ratio. The figures also show that when $\omega/\omega_{n<1}$ the ratio of dynamic stiffness to the static stiffness is less than unique except in big amount of damping ratio ($\rho>0.5$) which the ratio becomes more than 1. Finally for $\omega/\omega_{n>1}$, the ratio of dynamic to static stiffness rises rapidly and by increasing the additional mass, the value of dynamic stiffness in case of $\omega/\omega_{n>1}$ would increase highly.

CONCLUSION

Interaction of additional mass of soil with axial element in dynamic and seismic vibration case have rarely been considered by researchers. Combining the dynamic formulation distribution and dynamic experiments, one can find dynamic properties of a structure buried in soil like buried pipeline. Applying this model we can find the effect of static and dynamic parameters between soil and pipe to the factors like burial depth, pipe thickness, soil compaction, water absorption percentage, amplitude value and hysteric frequency. Some of the results can be concluded as:

- The static performance between soil and pipe is nonlinear in axial direction
- Increasing damping between soil and pipe, harmonic displacement phase delay and harmonic forces would rise up
- when the hysteric dominate grows, the value of force dominate between soil and pipe and dynamic stiffness would ascend
- 4-for $\omega<\omega_n$ ratio of dynamic stiffness to static stiffness is less than one. For very great amount of damping ratio, the ratio of dynamic to static stiffness becomes more than one
- 5-for $\omega>\omega_n$ the ratio of dynamic to static stiffness rises rapidly
- 6-by increasing damping ratio, the dynamic stiffness would increase too
- 7-when the additional mass grows the natural frequency decrease
- 8-dynamic stiffness increases when additional mass grows

REFRENCES

Do, H.L., B.H. Kim, H. Lee and J.S. Kong, 2009. Seismic behavior of a buried gas pipeline under earthquake excitations. Eng. Struct., 31: 1011-1023. DOI: 10.1016/J.ENGSTRUCT

Lee, L.N.H., 1984. Elastic-plastic buckling of buried pipelines by seismic excitation. Int. J. Soil Dyn. Earthquake Eng., 3: 168-173. DOI: 10.1016/0261-7277(84)90032-9

Manolis, G.D., P.I. Tetepoulidis, D.G. Talaslidis and G.A. Postolidis, 1995. Seismic analysis of buried pipeline in a 3D soil continuum. Eng. Anal. Bound. Elem., 15: 371-394. DOI: 10.1016/0955-7997(95)00035-M

Neil, T. and V. Tran, 1996. Experimental and theoretical studies in sub sea pipeline buckling. Mar. Struct., 9: 211-257. DOI: 10.1016/0951-8339(94)00021-J

Poulos, H.G. and K.B. Sim, 1979. Engineered piles to improve cyclic load capacity. Mar. Georesour. Geotechnol., 9: 131-140. DOI: 10.1080/10641199009388 235

Wang, L.R.L., J.S. Shim, I. Ishibashi and Y. Wang, 1990. Dynamic responses of buried pipelines during a liquefaction process. Soil Dyn. Earthquake Eng., 9: 44-50. DOI: 10.1016/S0267-7261(09)90009-4